



Co-doping effects and electrical transport in In–N doped zinc oxide

L.L. Chen^{a,b}, Z.Z. Ye^{a,*}, J.G. Lu^a, H.P. He^a, B.H. Zhao^a, L.P. Zhu^a,
Paul K. Chu^{b,*}, L. Shao^c

^a State Key Laboratory of Silicon Materials, Zhejiang University, Hangzhou 310027, People's Republic of China

^b Department of Physics and Materials Science, City University of Hong Kong, Tat Chee Avenue, Kowloon, Hong Kong, China

^c Los Alamos National Laboratory, Los Alamos, NM 87545, USA

Received 1 October 2006

Available online 18 October 2006

Abstract

The influence of indium concentrations on electrical properties of In–N co-doped ZnO thin films has been studied. Based on Hall-effect measurements and analyses, impurity scattering is the dominant mechanism determining the diminished mobility in ZnO with higher In concentration. X-ray photoelectron spectroscopy reveals that the presence of In enhances the solubility of N with the formation of In–N and Zn–N bonds. The optimal properties, namely resistivity of 16.1 Ω cm and Hall mobility of 1.13 $\text{cm}^2 \text{V}^{-1} \text{s}^{-1}$, are obtained at an indium concentration of 0.14 at.%. The diffraction angle of co-doped ZnO is closest to that of un-doped ZnO.

© 2006 Elsevier B.V. All rights reserved.

1. Introduction

Zinc oxide, with a direct band gap of 3.37 eV, has been attracting considerable attention because of promising applications in UV light-emitting diodes and diode lasers [1,2]. However, an obstacle hampering more widespread applications is that ZnO intrinsically shows n-type conductivity and it is difficult to dope the materials p-type. Nitrogen, a good p-type dopant in other II–VI semiconductors [3,4], has long been considered a possible p-type dopant in ZnO. Incorporation of both acceptors and reactive donors has been proposed to increase the solubility of N in ZnO [5], and experimental verification of co-doping in ZnO such as Al–N [6] and Ga–N [7] has been reported. Synthesis of p-type ZnO films with acceptable stability and reproducibility by means of indium and nitrogen co-doping has recently been demonstrated [8]. However, some fundamental properties such as the electrical transport in

co-doped ZnO is still not well understood. In this letter, results on our systematic study on the effects of co-doping and electrical transport properties in In–N co-doped ZnO films are described.

2. Experiments

ZnO films were synthesized on glass substrates by direct current (DC) reactive magnetron sputtering. $\text{In}_x\text{Zn}_{1-x}$ ($x = 0.05, 0.5, 0.8, 1, \text{ and } 5$ at.%) alloys (99.999% pure) were used as the co-doping targets. The deposition chamber was initially evacuated to a base pressure of 10^{-3} Pa and then a mixture of Ar (99.995%) and N_2O (99.99%) with a ratio of 1:1 was introduced as the sputtering gas to a total pressure of 4 Pa. The substrate temperature was maintained at 540 °C. Before deposition, the target was pre-sputtered for 10 min to remove surface contaminants. The sputtering time, current, and voltage were 30 min, 200 mA, and 200 V, respectively.

The film composition was determined by Rutherford backscattering spectrometry (RBS) using 2 MeV helium ions and a Si barrier detector located at a backscattering angle of 167°. The RBS spectra were fitted using SIMNRA

* Corresponding authors. Fax: +86 571 87952625 (Z.Z. Ye); +852 27889549 (Paul K. Chu).

E-mail addresses: yezz@zju.edu.cn (Z.Z. Ye), paul.chu@cityu.edu.hk (P.K. Chu).

which is a common simulation program for MeV ion beam analysis of backscattering spectra [9]. The electrical properties were measured by Hall-effect measurements using the Van der Pauw configuration system (BIO-RAD HL5500PC) at room temperature. The chemical bonding states of nitrogen and indium in the films were characterized by X-ray photoelectron spectroscopy (XPS) [VG ESCALAB MK-II, Mg $K\alpha$ source]. The crystal structure was determined by X-ray diffraction (XRD) on the Thermo ARL X'TRA with Cu $K\alpha$ radiation ($\lambda = 0.154056$ nm).

3. Results and discussion

Fig. 1 shows the variation of the In concentrations in the films versus those in the targets as determined by RBS. The insert shows the SIMNRA fit for a typical RBS spectrum. The thickness of the as-grown In–N co-doped ZnO thin films is 120–150 nm. On account of the relative low sensitivity of N by RBS, it is difficult to accurately determine the N concentration in the films. Fig. 1 shows that the In concentrations in the films are proportional to those in the targets within 1 at.%, but the In to Zn ratios in the films are not necessarily the same as those in the targets.

Fig. 2 shows the dependence of the electrical properties on In concentrations for the In–N co-doped ZnO films. The films with In concentrations below 0.25 at.% exhibit p-type conductivity. Among these samples, the film with an In content of 0.02 at.% exhibits high resistivity and low carrier concentration. As the In concentration increases, the p-type conductivity is enhanced. The optimal results, namely resistivity of $16.1 \Omega \text{ cm}$, carrier concentration of $3.42 \times 10^{17} \text{ cm}^{-3}$, and Hall mobility of $1.13 \text{ cm}^2 \text{ V}^{-1} \text{ s}^{-1}$, are observed when the In concentration in the film is 0.14 at.%. Further increases in the In concentrations lead to gradually rising resistivity. When In concentration reaches 0.51 at.%, a rather high resistivity and ambiguous carrier type are observed. In our measurements, only the Hall voltage magnitude and sign are definite for the sample. Due to the ambiguity, the carrier concentration

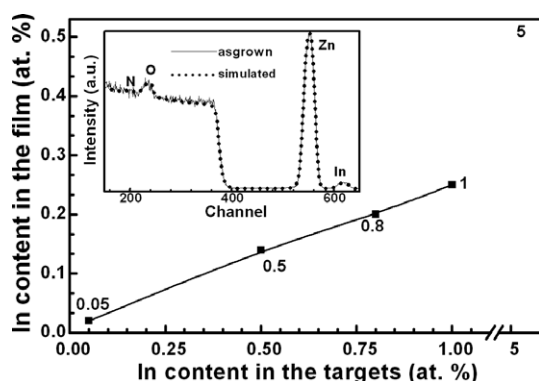


Fig. 1. Relationship between In concentrations in the co-doped ZnO films with those in the sputtering targets. The inset shows the random RBS spectrum of the film with an In concentration of 0.51 at.%. The dotted curve shows the excellent SIMNRA fit.

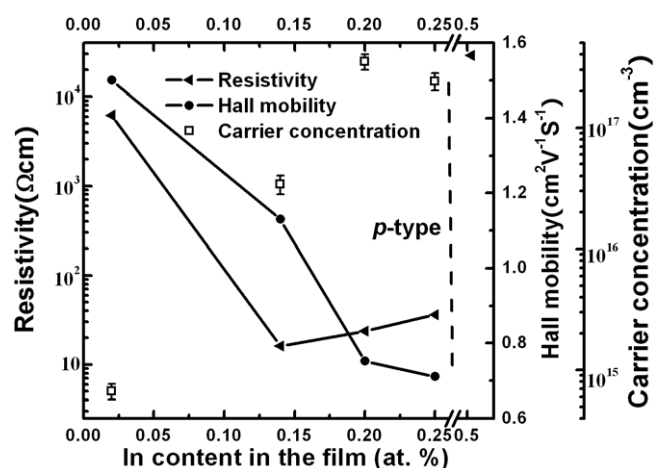


Fig. 2. Dependence of electrical properties of In–N co-doped ZnO films on In concentrations.

and Hall mobility of the sample doped with 0.51 at.% In are not included in the plots. Our results also indicate that the mobility in the films decrease with increasing In contents.

In order to determine the dominant scattering mechanism for the mobility variation, we consider grain boundary scattering, lattice scattering, and ion impurity scattering. To estimate the contribution of grain boundary scattering, the mean free paths of the carriers in the films are calculated using [10]

$$l = \left(\frac{h}{2e} \right) \left(\frac{3n}{\pi} \right)^{1/3} \mu, \quad (1)$$

where μ is the charge carrier mobility and n is the carrier concentration. The calculated results are in the range of 0.26–1.61 nm, which is much smaller than the crystalline size of the ZnO film (120–150 nm), suggesting that the contribution from the grain boundary scattering mechanism can be neglected. As for the lattice scattering mechanism, it is only evident at high temperatures. Since the Hall-effect measurements are carried out at room temperature, lattice scattering should not be the dominant scattering mechanism. In addition, according to the Conwell–Weisskopf formula, when degenerate charge carriers are scattered by impurity ions, the mobility can be described as [11,12]

$$\mu_i = \left(\frac{2}{m^*} \right)^{1/2} \frac{\varepsilon^{1/2} E_F^{3/2}}{\pi e^3 N_i Z^2} \frac{1}{\ln \left(1 + \frac{\varepsilon E_F}{N_i^{1/3} Z e^2} \right)}, \quad (2)$$

where m^* is the effective mass of electrons, ε is a static dielectric constant of the films, E_F is the Fermi energy level, and N_i is the concentration of the scattering centers. Hence, a high doping concentration will lead to a larger population of ionized impurities, consequently leading to decreased mobility with higher In concentrations. We believe that this is the dominant mechanism for our observed mobility variation.

To further investigate the mechanism, X-ray photoelectron spectroscopy (XPS) was performed to examine the chemical states of In and N in the ZnO films. The XPS spectra of the ZnO film with 0.14 at.% In are depicted in Fig. 3. The In $3d_{5/2}$ (443.4 eV) and In $3d_{3/2}$ (451.1 eV) peaks in Fig. 3a indicate In–O or In–N bonds [13]. The N1s spectrum in Fig. 3b is deconvoluted numerically with Gaussian functions into two components with peak energies of 397.3 eV and 396.0 eV. The peak at 397.3 eV can be attributed to N–In bonds based on the fact that a similar peak has been observed from GaN thin films (397.1 eV) [14]. The peak at 396.0 eV is related to Zn–N bonds (N_O) [15], which are believed to contribute to the good p-type behavior as demonstrated by the Hall-effect measurements. Thus, it is very reasonable to conclude that the presence of In enhances the incorporation of N via the formation of In–N and Zn–N bonds. It should also be noted that for the In–N co-doped ZnO films, there is significant scattering from neutral impurities as well as ionized impurities. With increasing In concentrations, more InN acts as defects and scattering centers in the films thereby adversely affecting the mobility. This is consistent with the mobility trend shown in Fig. 2.

Although the tendency of the decreasing mobility can be explained, it is more difficult to fathom why the optimal electrical properties are achieved when the materials are doped with a certain amount of In. Fig. 4 displays the XRD patterns acquired from three of the In–N co-doped ZnO films. All the films show only the (002) Bragg peaks and no Zn_3N_2 , In_2O_3 , or InN peaks can be detected. The results suggest a high *c*-axis orientation and satisfactory crystal quality. With increasing In concentrations, the

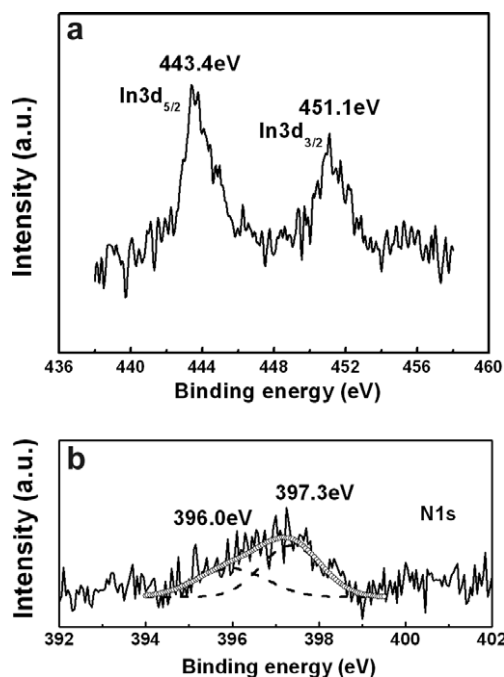


Fig. 3. XPS spectra obtained from the co-doped ZnO having an In concentration of 0.14 at.%: (a) In3d, (b) N1s.

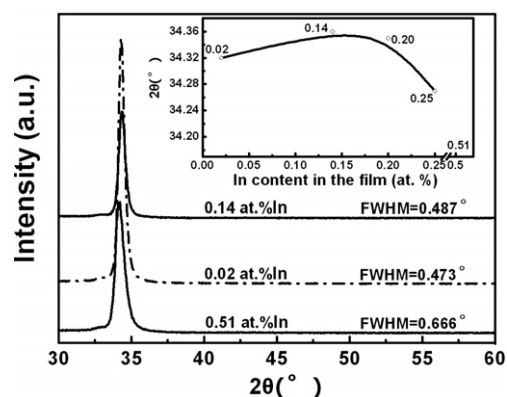


Fig. 4. XRD spectra acquired from the co-doped ZnO films with In concentrations of 0.02, 0.14, and 0.51 at.%. The inset shows the relationship between the diffraction angle of the (002) peak and In concentrations.

FWHM (full width at half maximum) value of the (002) peak increases, implying degraded crystallinity due to incorporation of In and N atoms. The diffraction angles of the (002) peaks are shown in the inset of Fig. 4. They shift to higher values initially with increasing In concentrations. The maximum diffraction angle of 34.36° is observed from the sample having an In concentration of 0.14 at.%. Further increases in the In concentration lead to smaller diffraction angles. The maximum diffraction angle of 34.36° determined from the co-doped ZnO films is close to that of un-doped ZnO (34.37°). This experimental result suggests that no evident strain or inclusion-induced lattice distortion has been developed in the ZnO film when the In concentration is 0.14 at.%. Simultaneous incorporation of appropriate concentration of N and In introduces offsetting local lattice expansion and contraction, subsequently minimizing the lattice strain and improving the electrical characteristics. In addition, this allows the N acceptor to exist in a stable state. The stability of N can also be understood by the reduction in the Madelung energy for co-doping [16]. Based on the two major scattering mechanisms involving ion and neutral impurities that affect the mobility, co-doped p-type ZnO thin films with both high carrier concentration and high mobility are difficult to obtain at the same time and there should exist a certain In to N concentration ratio that yields the optimal characteristics. Our results indicate that it occurs when the diffraction angle is closest to that of un-doped ZnO.

4. Conclusions

In summary, the influence of the indium doping concentration on the electrical properties of In–N co-doped ZnO thin films has been systematically studied. Based on Hall-effect measurements and analyses, impurity scattering is the dominant mechanism for the diminished mobility with higher In concentrations. XPS reveals that the presence of In enhances the solubility of N with the formation of In–N and Zn–N bonds. The optimal properties, namely resistiv-

ity of $16.1 \Omega \text{ cm}$ and Hall mobility of $1.13 \text{ cm}^2 \text{ V}^{-1} \text{ s}^{-1}$, are obtained when the indium concentration is 0.14 at.% and the diffraction angle of co-doped ZnO is closest to that of un-doped ZnO.

Acknowledgements

This work was jointly supported by “973” Program of China under Grant No. 2006CB604906, National Natural Science Foundation of China Under Grant No. 50532060 and No. 60340460439, Zhejiang Provincial Natural Science Foundation of China Under Grant No. Y405126, and City University of Hong Kong Direct Allocation Grant No. 9360110.

References

- [1] X.-L. Guo, J.-H. Choi, H. Tabata, T. Kawai, *Jpn. J. Appl. Phys.* 40 (2001) L177.
- [2] H. Cao, Y.G. Zhao, S.T. Ho, E.W. Seelig, Q.H. Wang, R.P.H. Chang, *Phys. Rev. Lett.* 82 (1999) 2278.
- [3] K. Ohkawa, T. Karasawa, T. Mitsuyu, *Jpn. J. Appl. Phys.* 30 (1991) L152.
- [4] R.M. Park, M.B. Troffer, C.M. Rouleau, J.M. DePuydt, M.A. Haase, *Appl. Phys. Lett.* 57 (1990) 2127.
- [5] T. Yamamoto, H.K. Yoshida, *Physica B* 302/303 (2001) 55.
- [6] J.G. Lu, Z.Z. Ye, F. Zhuge, Y.J. Zeng, B.H. Zhao, L.P. Zhu, *Appl. Phys. Lett.* 85 (2004) 3134.
- [7] M. Joseph, H. Tabata, T. Kawai, *Jpn. J. Appl. Phys. Part 2* 38 (1999) L1205.
- [8] L.L. Chen et al., *Appl. Phys. Lett.* 87 (2005) 252106.
- [9] Available from <<http://www.rzg.mpg.de/~mam/>>.
- [10] M. Chen, Z.L. Pei, X. Wang, Y.H. Yu, X.H. Liu, C. Sun, L.S. Wen, *J. Phy. D: Appl. Phys.* 33 (2000) 2538.
- [11] J. Ma, F. Ji, D.H. Zhang, H.L. Ma, S.Y. Li, *Thin Solid Films* 357 (1999) 98.
- [12] W. Tang, D.C. Cameron, *Thin Solid Films* 238 (1994) 83.
- [13] M. Procop, *J. Electron Spectrosc. Relat. Phenom.* 59 (1992) R1.
- [14] R. Carin, J.P. Deville, J. Werckmann, *Surf. Interf. Anal.* 16 (1990) 65.
- [15] M. Futsuhara, K. Yoshioka, O. Takai, *Thin Solid Films* 322 (1998) 274.
- [16] T. Yamamoto, H. Katayama-Yoshida, *Jpn. J. Appl. Phys.* 38 (1999) L166.